ResearchGate

See discussions, stats, and author profiles for this publication at: https://www.researchgate.net/publication/233972200

Dynamical growth behavior of copper clusters during electrodeposition

Article *in* Applied Physics Letters · July 2010

DOI: 10.1063/1.3464550

CITATIONS
14

READS
59

7 authors, including:

Yong S Chu
Brookhaven National Laboratory
268 PUBLICATIONS **4,178** CITATIONS

SEE PROFILE

Jaemock Yi
Samsung Advanced Institute of Technology
32 PUBLICATIONS **725** CITATIONS

SEE PROFILE

G. Margaritondo
École Polytechnique Fédérale de Lausanne
1,059 PUBLICATIONS **17,247** CITATIONS

SEE PROFILE

Some of the authors of this publication are also working on these related projects:

Project Nano-positioning View project

Project Electronic Structure of High Temperature Superconductors View project

All content following this page was uploaded by Yong S Chu on 16 May 2014.

The user has requested enhancement of the downloaded file.

Dynamical growth behavior of copper clusters during electrodeposition

Pei-Cheng Hsu,[1] Yong Chu,[2] Jae-Mock Yi,[2] Cheng-Liang Wang,[1] Syue-Ren Wu,[1,3] Y. Hwu,[1,3,4,a)] and G. Margaritondo[5]
[1]*Institute of Physics, Academia Sinica, Taipei 115, Taiwan*
[2]*Advanced Photon Source, Argonne National Laboratory, Argonne, Illinois 60439, USA*
[3]*Department of Engineering Science and System, National Tsing Hua University, Hsinchu 300, Taiwan*
[4]*Institute of Optoelectronic Sciences, National Ocean University, Keelung 202, Taiwan*
[5]*Ecole Polytechnique Fédérale de Lausanne (EPFL), CH-1015 Lausanne, Switzerland*

(Received 20 May 2010; accepted 23 June 2010; published online 19 July 2010)

Ultrahigh resolution full-field transmission x-ray microscopy enabled us to observe detailed phenomena during the potentiostatic copper electrodeposition on polycrystalline gold. We detected two coexisting cluster populations with different sizes. Their growth behaviors are different, with a shape transitions only occurring for large clusters. These differences influence the micromorphology and general properties of the overlayer. © *2010 American Institute of Physics*. [doi:10.1063/1.3464550]

Electrodeposition, widely used for industrial coatings,[1] is potentially very interesting for nanotechnology because of its site-specificity and easily tunable parameters. Specifically, copper electrodeposition finds interesting applications in electronic devices.[2] However, insufficient understanding of the initial growth hampers the exploitation of nanoscale electrodeposition[3] and imposes empirical solutions for problems such as grain size effects.

Our present work exploits the power of full-field transmission x-ray microscopy (TXM) to reveal important details of the initial Cu growth. We observe two cluster populations with very different sizes, reminiscent of other copper electrodeposition processes,[4–6] especially in high aspect ratio trenches.[7,8] This can impact the conductivity, reliability, and overall performance of the corresponding nanotechnology devices.

Most previous studies of Cu electrodeposition used electrochemical measurements and *ex situ* imaging[9–14] plus theoretical growth models.[15] Scanning electron microscopy and atomic force microscopy could be used for "stop-and-go" observations, not optimized to study growth dynamics. Ultrahigh-resolution scanning probe microscopy provided important information on surface defects[16–23] but limited facts on growth dynamics. Transmission electron microscopy in a liquid environment[3,24,25] investigated Cu nucleation with results divergent from theory.

In our study, ultrahigh-resolution TXM offers several advantages: it analyzes electrodeposition in a realistic electrochemical environment thanks to its penetration depth and quantitatively monitors the growth. Its present performances[26] (30 nm lateral resolution, 50 ms time resolution, phase contrast enhancement) can reveal nanoscale details and fast growth dynamics.

Such performances were essential for obtaining our main result. We observed not only two coexisting cluster population but also marked differences in their growth behavior. For example, clusters of the "large size" population grow without other clusters nearby. They grow more rapidly than the "small-size" population and their shape changes during growth.

The smaller clusters grow instead at densely distributed nucleation sites and neighboring clusters limit their growth rate. This also restricts the rate of thickness increase. Contrary to large clusters, their shape remains unchanged during growth.

We performed the experiments in a specially designed miniature cell consisting of two silicon wafers coated with a 1 μm silicon nitride layer, separated by a 200 μm thick silicon wafer. Each lateral wafer was etched to create a 2×2 mm^2 silicon nitride window transparent to x-ray. On such windows, we fabricated the cathode and the anode by evaporating 50 nm gold on a 10 nm chromium adhesion layer.

The electrodeposition solution was 0.25 M analytical-grade copper sulfate in deionized water. The deposition was performed at room temperature with an Autolab potentiostat-galvanostat PGSTAT 30.

The TXM studies were performed at the 32-ID microscopy beamline of the advanced photon source, Argonne National Laboratory and at the 01B beamline of the Taiwan National Synchrotron Radiation Research Center. Our full-field TXM uses a set of capillary condensers to shape the monochromatic x-ray beam and focus it on the object. The magnifying element is an Au zone plate with 30 nm outermost zone width and 450 nm thickness.

The theoretical background for our results was Scharifker and Hill's work on the nucleation for diffusion controlled growth.[15] They identified two processes: instantaneous growth and progressive growth. If the nucleation rate is faster than the cluster growth rate, then nucleation occurs at all sites in a very short time, almost instantaneously. If the contrary is true, then nucleation at additional sites continues to occur while the previously nucleated clusters grow leading to progressive growth.

For instantaneous growth, the theoretical current i versus time t function is the following:

a)Author to whom correspondence should be addressed. Electronic mail: phhwu@sinica.edu.tw.

 © 2010 American Institute of Physics

Downloaded 17 Oct 2010 to 130.199.3.130. Redistribution subject to AIP license or copyright; see http://apl.aip.org/about/rights_and_permissions

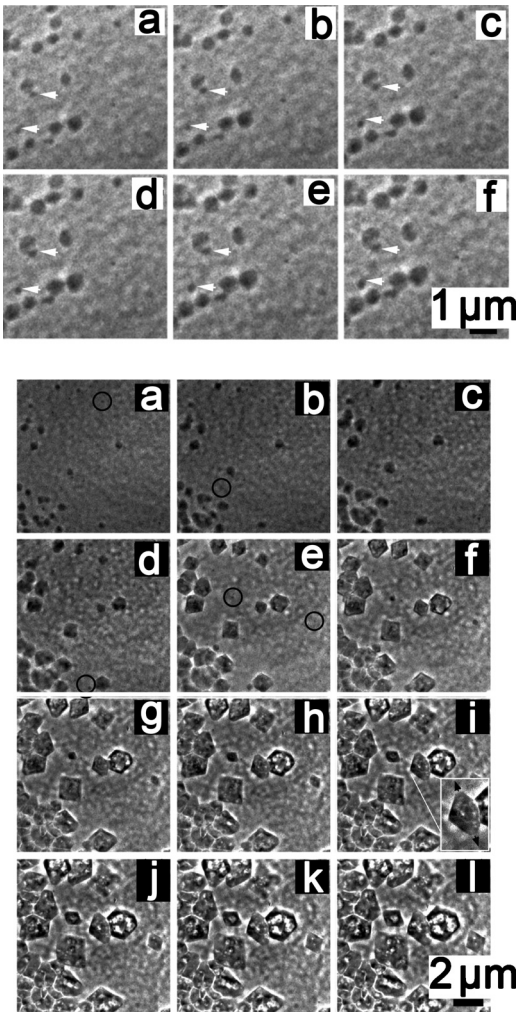

FIG. 1. Top: TXM images during Cu deposition at −1 V, taken at (a) 60, (b) 70, (c) 80, (d) 90, (e) 100, and (f) 110 s. The white arrows mark additional nucleated clusters. Bottom: TXM images similar to the previous ones but taken over a longer time period: (a) 60, (b) 100, (c) 140, (d) 180, (e) 220, (f) 260, (g) 300, (h) 340, (i) 380, (j) 420, (k) 460, and (l) 500 s. The images show two different cluster populations with different sizes and growth behavior.

$$\left(\frac{i}{i_{\max}}\right)^2 = 1.9542\left(\frac{t_{\max}}{t}\right)\left\{1-\exp\left(-1.2564\frac{t}{t_{\max}}\right)\right\}^2,$$

where $i_{\max}$ and $t_{\max}$ are the maximum values. For progressive nucleation, the function is instead the following:

$$\left(\frac{i}{i_{\max}}\right)^2 = 1.2254\left(\frac{t_{\max}}{t}\right)\left\{1-\exp\left(-2.3367\frac{t}{t_{\max}}\right)\right\}^2.$$

These predictions were fitted to our experimental data obtaining a good result with the progressive-growth model but only in the initial growth stage and then significant deviations. This indicates that the actual growth is more complex.

Figure 1 (top) shows TXM images during the first growth stage. Nucleation does not immediately occur after applying the −1 V potential, again indicating progressive growth. After a certain time, clusters with uniform size appear at random sites. Additional clusters are then nucleated (white arrows in Fig. 1, top) while previously nucleated cluster continue to grow.

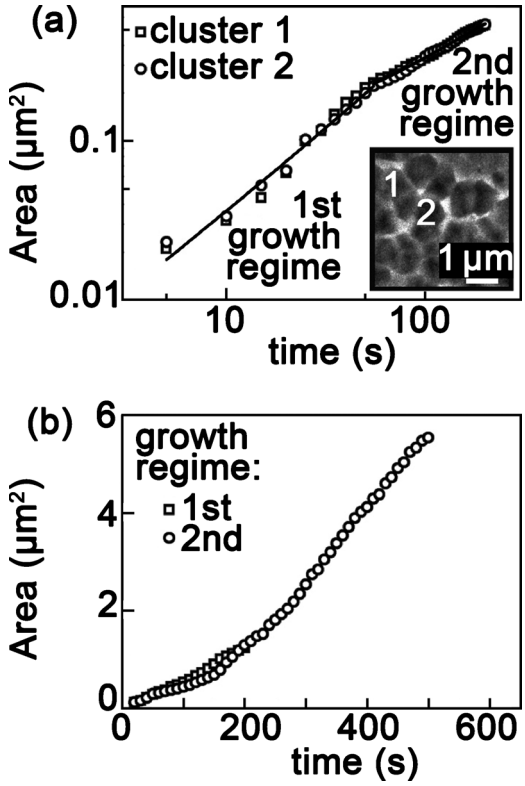

FIG. 2. Cluster area vs time. (a) Data for two different clusters (seen in the TXM image of the inset), both belonging to the "small size" population. (b) Data from two different regions corresponding to the large-size and small-size populations.

As electrodeposition progresses, we observe (Fig. 1, bottom) two populations of clusters with different sizes. The smaller clusters grow at densely packed sites and their growth rate decreases gradually. Eventually, they form multifaceted three-dimensional agglomerates that merge with their neighbors achieving complete surface coverage (lower left part of Fig. 1, bottom).

The base area versus time plots of Fig. 2(a), reveal two growth regimes for these smaller clusters. The second regime starts when the clusters begin to touch each other and the growth rate decreases. This is reasonable since with decreased intercluster areas the supply of copper ions to the surface is reduced.

The large-size clusters in Fig. 1 (bottom) initially grow without neighbors, rapidly expanding until they touch each other. Their initial shape is square-based pyramidal but then becomes hexagonal-based pyramidal as the growth rate increases. Such conclusions about cluster shapes were confirmed by tomographically reconstructed TXM images, Fig. 3, that also yields the cluster thickness. For small-size clusters, after complete coverage the thickness is ~0.2 μm. For the large-size population, the thickness is ~1 μm.

The cluster thickness was also derived from the oscillation versus time of the cluster TXM image intensity due to Zernike contrast and to the dependence on thickness of the phase shift. The results confirm and corroborate the above conclusions.

The direct observation of two cluster populations with different growth properties emphasizes the importance of direct microscopy studies of growth dynamics. Transport measurements only provide average information in the present case, mixing the features of the two cluster populations. This

Downloaded 17 Oct 2010 to 130.199.3.130. Redistribution subject to AIP license or copyright; see http://apl.aip.org/about/rights_and_permissions

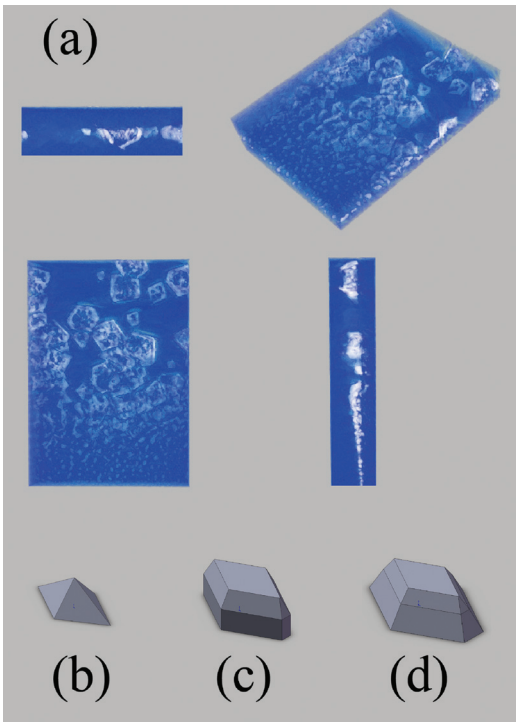

FIG. 3. (Color) (a) Tomographically reconstructed TXM images showing the different cluster shapes, pictured in the bottom: (b) square-based pyramidal; (c) intermediate; (d) hexagonal-based pyramidal.

misses the detailed growth features that can play an important role in the final device performances.

This work was supported by the National Science Council, by the Academia Sinica, by the National Science and Technology Program for Nanoscience and Nanotechnology (Taiwan), by the Swiss Fonds National de la Research Scientifique, and by the EPFL Center for Biomedical Imaging (CIBM). The use of the Advanced Photon Source is supported by the U.S. Department of Energy, Office of Sciences, Office of Basic Energy Sciences, under Contract No. DE-AC0206CH111357.

[1]*Electrocatalysis: Computational, Experimental, and Industrial Aspects*, edited by C. F. Zinola (CRC, Boca Raton, 2010).
[2]P. C. Andricacos, C. Uzoh, J. O. Dukovic, J. Horkans, and H. Deligianni, IBM J. Res. Dev. **42**, 567 (1998).
[3]A. Radisic, P. M. Vereecken, J. B. Hannon, P. C. Searson, and F. M. Ross, Nano Lett. **6**, 238 (2006).
[4]C. H. Seah, S. Mridha, and L. H. Chan, J. Vac. Sci. Technol. B **17**, 2352 (1999).
[5]M. T. Pérez-Prado and J. J. Vlassak, Scr. Mater. **47**, 817 (2002).
[6]L. Guo, A. Radisic, and P. C. Searson, J. Electrochem. Soc. **153**, C840 (2006).
[7]K. Mirpuri and J. Szpunar, Micron **35**, 575 (2004).
[8]T. P. Moffat, M. Walker, P. J. Chen, J. E. Bonevich, W. F. Egehoff, L. Richter, C. Witt, T. Aaltonen, M. Ritala, M. Leskela, and D. Josell, J. Electrochem. Soc. **153**, C37 (2006).
[9]C. Ji, G. Oskam, and P. C. Searson, J. Electrochem. Soc. **148**, C746 (2001).
[10]D. Grujicic and B. Pesic, Electrochim. Acta **47**, 2901 (2002).
[11]A. Radisic, Y. Cao, P. Taephaisitphongse, A. C. West, and P. C. Searson, J. Electrochem. Soc. **150**, C362 (2003).
[12]L. Magagnin, A. Vicenzo, M. Bain, H. W. Toh, H. S. Gamble, and P. L. Cavallotti, Microelectron. Eng. **76**, 131 (2004).
[13]T. Zapryanova, A. Hrussanova, and A. Milchev, J. Electroanal. Chem. **600**, 311 (2007).
[14]W. Shao, G. Pattanaik, and G. Zangari, J. Electrochem. Soc. **154**, D339 (2007).
[15]B. Scharifker and G. Hill, Electrochim. Acta **28**, 879 (1983).
[16]O. M. Magnussen, J. Hotlos, R. J. Nichols, D. M. Kolb, and R. J. Behm, Phys. Rev. Lett. **64**, 2929 (1990).
[17]S. Manne, P. K. Hansma, J. Massie, V. B. Elings, and A. A. Gewirth, Science **251**, 183 (1991).
[18]N. Batina, D. M. Kolb, and R. J. Nichols, Langmuir **8**, 2572 (1992).
[19]J. E. T. Andersen and P. Moller, J. Electrochem. Soc. **142**, 2225 (1995).
[20]M. H. Hölzle, C. W. Apsel, T. Will, and D. M. Kolb, J. Electrochem. Soc. **142**, 3741 (1995).
[21]M. H. Hölzle, V. Zwing and D. M. Kolb, Electrochim. Acta **40**, 1237 (1995).
[22]R. M. Rynders and R. C. Alkire, J. Electrochem. Soc. **141**, 1166 (1994).
[23]W. U. Schmidt, R. C. Alkire, and A. A. Gewirth, J. Electrochem. Soc. **143**, 3122 (1996).
[24]M. J. Williamson, R. M. Tromp, P. M. Vereecken, R. Hull, and F. M. Ross, Nature Mater. **2**, 532 (2003).
[25]A. Radisic, P. M. Vereecken, P. C. Searson, and F. M. Ross, Surf. Sci. **600**, 1817 (2006).
[26]Y. S. Chu, J. M. Yi, F. De Carlo, Q. Chen, W. K. Lee, H. J. Wu, C. L. Wang, J. Y. Wang, C. J. Liu, C. H. Wang, S. R. Wu, C. C. Chien, Y. Hwu, A. Tkachuk, W. Yun, M. Feser, K. S. Liang, C. S. Yang, J. H. Je, and G. Margaritondo, Appl. Phys. Lett. **92**, 103119 (2008).

Downloaded 17 Oct 2010 to 130.199.3.130. Redistribution subject to AIP license or copyright; see http://apl.aip.org/about/rights_and_permissions
View publication stats